



Radiation of moving sources in time-domain simulations of outdoor sound propagation

Didier Dagna, Thomas Bontemps and Philippe Blanc-Benon

Laboratoire de Mécanique des Fluides et d'Acoustique, UMR CNRS 5509, École Centrale de Lyon, Université de Lyon, 36 Avenue Guy de Collongue, 69134 Ecully Cedex, France.

Summary

This paper is concerned with time-domain simulations of radiation of moving sources in complex outdoor environments. Indeed, time-domain methods are well-adapted to study the radiation of moving sources as they can handle any source trajectory and any variation of the source speed during its motion. The case of a source moving at a constant height and at a constant speed above a flat ground is examined. First, the numerical solution is compared with an analytical solution for a perfectly reflecting ground. Results are then examined for a finite-impedance ground. An extension of a recently proposed analytical solution for a 2-D geometry is proposed and a comparison of the obtained solution is performed with the numerical solution.

PACS no. 43.20.Ef, 43.28.Js, 43.28.En

1. Introduction

Time-domain methods are now mature to investigate complex problems in outdoor sound propagation in large three-dimensional geometries [1, 2, 3]. In particular, they allow us to study the acoustic field generated by moving sources in realistic environments, which is not available using frequency-domain methods. The feasibility of time-domain numerical simulations of radiation of moving sources have been shown recently in [4, 5].

The paper is concerned with the radiation of a monopole moving above an impedance plane at a constant speed at a constant height. This is a canonical problem for radiation of sources in motion and has been investigated analytically by many authors [6, 7]. However, it was noticed by Ochmann [8] that all the proposed analytical solutions assume that the surface impedance does not vary with the frequency during the motion of the source. An analytical solution has been proposed recently in [9] for a line source moving at a constant speed and at a constant height above an impedance plane which removes this assumption. In particular, it was shown that for sources moving close to the ground and at a Mach number higher than 0.2 a significant error could be obtained.

The objective of the paper is to compare the numerical solution obtained from a time-domain solver

of the linearized Euler equations to analytical solutions. In particular, an analytical solution for a finite-impedance ground surface which accounts for the frequency variation of the impedance during the motion of the source is proposed.

The paper is organized as follows. In Sec. II, the problem is described and the parameters of the numerical simulation are given. The case of a perfectly reflecting surface is then studied in Sec. III and the numerical solution is compared to an analytical solution. In Sec. IV, an impedance surface is considered. The numerical solution is first presented and an analytical solution is proposed.

2. Description of the problem

The radiation of a monopole moving at a constant height and at a constant speed above an impedance plane is investigated. The scheme of the problem is depicted in Fig. 1.

The linearized Euler equations are solved using optimized high-order finite-difference schemes. At the outer boundaries, Perfectly Matched Layers [10] are employed. At the ground, a time-domain impedance boundary condition [11] is implemented. The solver is presented in [12].

The grid is Cartesian with $2001 \times 351 \times 72$ points in the x -, y - and z -directions, respectively. The spatial step is uniform with $\Delta x = \Delta y = \Delta z = 0.1$. The time step is set to 2.9×10^{-4} s and 12000 time iterations are performed.

The moving source is implemented through the mass source term:

$$S(\mathbf{x}, t) = s(t)Q(\mathbf{x} - \mathbf{x}_S - \mathbf{V}_0 t), \quad (1)$$

where $\mathbf{x}_S = (0, 0, z_S)$ with $z_S = 2.1$ m and with $\mathbf{V}_0 = (V_0, 0, 0)$. The Mach number $M = V_0/c_0$ is equal to 0.15. The source spatial distribution $Q(\mathbf{x})$ is Gaussian and its halfwidth is equal to 0.1 m. The signal $s(t)$ is constructed by filtering a white noise signal by a Gaussian centered at 300 Hz and whose halfwidth is approximately equal to 100 Hz. Note that the mean value of the time-frequency decompositions of the acoustic pressure presented in the following sections are obtained by averaging the value obtained for ten realizations of the signal $s(t)$. The acoustic pressure obtained at a receiver located at $x = 0$ m, $y = 4.9$ m and $z = 3$ m is studied hereafter.

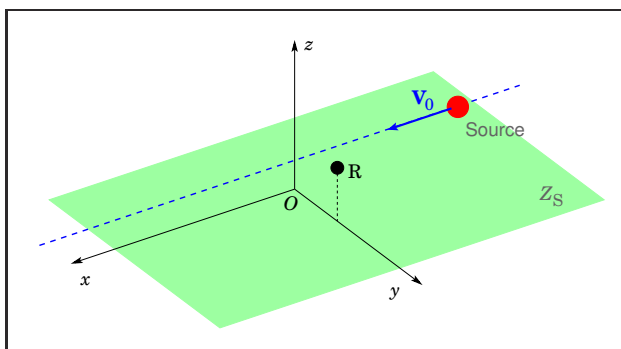


Figure 1. Source moving at a constant speed above an impedance plane.

Two types of ground surface are investigated: the first one is a perfectly reflecting surface and the second one is an absorbing surface. For that, an impedance plane is considered, using the Miki model [13] of a semi-infinite ground of air flow resistivity 100 kPa s m^{-2} .

3. Results for a perfectly reflecting ground

3.1. Numerical solution

First, a perfectly reflecting surface is considered. The time-frequency decomposition of the acoustic pressure, corresponding to a short-time power spectral density (PSD) of the pressure, at the receiver is shown in Fig. 2. It is observed that the frequency contents of the acoustic pressure is between 300 and 500 Hz as the sources approaches the receiver ($t < 0$) and is between 200 and 400 Hz as the source recedes from the receiver ($t > 0$). This is obviously related to the Doppler shift. Close to the receiver, the power spectral density presents destructive interference patterns, for which the PSD becomes very small. The location

of these interferences can be obtained analytically as for a non-moving source [4] and are plotted as dashed lines in Fig. 2. A good agreement is obtained.

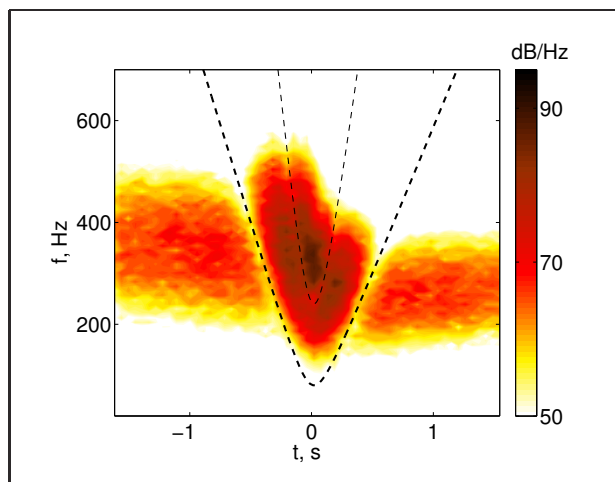


Figure 2. Time-frequency decomposition of the acoustic pressure at the receiver obtained from the numerical solution for a perfectly reflecting ground. Extract from [4].

3.2. Comparison to an analytical solution

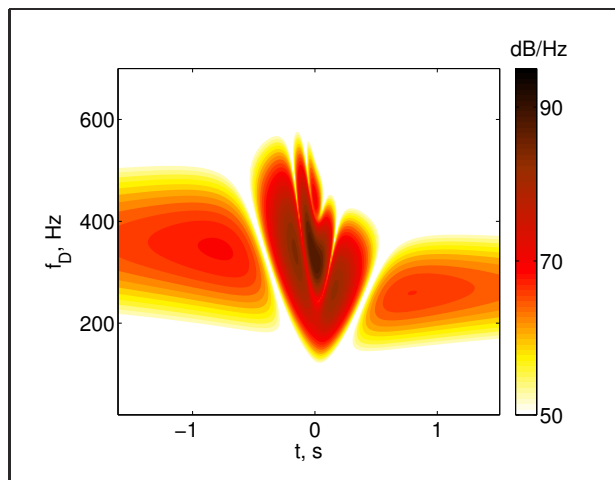


Figure 3. Time-frequency decomposition of the acoustic pressure at the receiver obtained from the analytical solution for a perfectly reflecting ground. Extract from [4].

The PSD obtained in the previous section is compared to that obtained from an analytical solution. For a perfectly reflecting surface, the analytical solution is the sum of two contributions, one from the source and the other from the image source located symmetrically with the respect to the ground plane to the source. Therefore, the PSD of the acoustic pressure is obtained from:

$$\text{PSD}[p](\mathbf{x}, f, t) = \text{PSD}[s](f) \hat{Q}(k_D) \rho_0^2 c_0^2 |G(\mathbf{x}, f, t)|^2, \quad (2)$$

where $\text{PSD}[s]$ is the PSD of the source signal $s(t)$ and where the Green's function is given by :

$$G(\mathbf{x}, f, t) = ik \left(\frac{e^{ikR_{e,1}}}{4\pi R_{e,1}(1 - M \cos \theta_{e,1})^2} + \frac{e^{ikR_{e,2}}}{4\pi R_{e,2}(1 - M \cos \theta_{e,2})^2} \right), \quad (3)$$

with $k = \omega/c_0$ and $\omega = 2\pi f$. The parameters $(R_{e,1}, \cos \theta_{e,1})$ and $(R_{e,2}, \cos \theta_{e,2})$ correspond to the retarded time coordinates centered at the source and at the image source, respectively. In addition, the term $\hat{Q}(k_D)$ is the spatial Fourier transform of the source spatial distribution Q evaluated at the wavenumber $k_D = k/(1 - M \cos \theta_{e,1})$ and accounts for the non-compactness of the source.

The PSD of the pressure obtained analytically is plot in Fig. 3 as a function of the time and the frequency. Compared to the numerical solution in Fig. 2, it appears smoother as the source signal in the numerical solution is obtained from a random signal. However, it is observed that a very good agreement between the two solutions is found. A quantitative comparison has also been performed in [4], showing that the deviations for a short-time equivalent sound pressure level were lower than 0.5 dB.

4. Results for an absorbing surface

4.1. Numerical solution

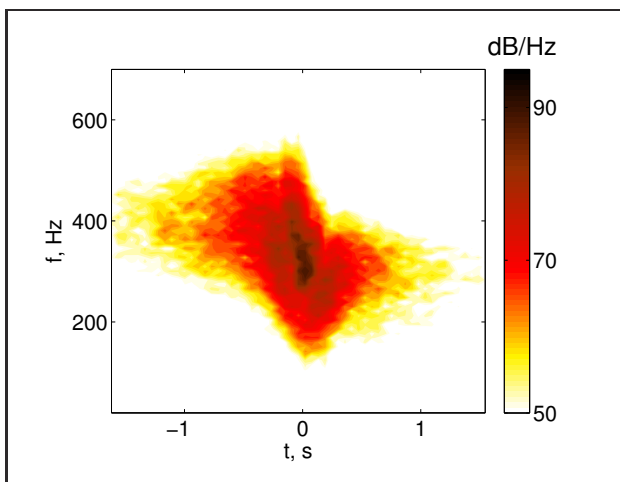


Figure 4. Time-frequency decomposition of the acoustic pressure at the receiver obtained from the numerical solution for an absorbing ground. Extract from [4].

The numerical solution obtained for an absorbing surface is depicted in Fig. 4. It is dramatically different to that obtained for a perfectly reflecting surface in Fig. 2. Indeed, the PSD of the acoustic pressure is approximately 20 dB lower than that obtained for a

perfectly reflecting surface as the source is far from the receiver ($|t| > 0.7$ s). In addition, the strong destructive interference pattern remarked in Fig. 2 does not appear for this absorbing surface. The Doppler effect is still observed as the maximum of the PSD is obtained for a frequency close to 400 Hz as the source approaches the receiver and for a frequency close to 300 Hz as the source recedes from the receiver.

4.2. Comparison to an analytical solution

The numerical solution presented in the previous paragraph is now compared to an analytical solution. This solution is an extension of that proposed recently for the sound radiation of a harmonic line source above an impedance ground plane [9]. Analytical solutions [6, 7] have already been proposed for this problem, but do not account for the frequency variation of the surface impedance during the motion of the source.

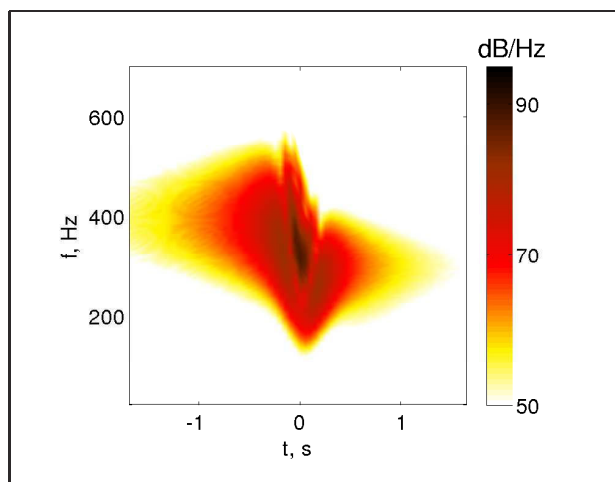


Figure 5. Time-frequency decomposition of the acoustic pressure at the receiver obtained from the analytical solution for an absorbing ground.

As usually done for this problem, the analytical solution is given in the Lorentz space. Coordinates are obtained from those in the physical space by the equations:

$$x_L = \gamma^2(x - Mc_0t), \quad (4)$$

$$y_L = \gamma y, \quad (5)$$

$$z_L = \gamma z, \quad (6)$$

$$t_L = \gamma^2(t - Mx/c_0), \quad (7)$$

with $\gamma = 1/\sqrt{1 - M^2}$. In the Lorentz space, the Green's function can be sought under the form $G = \tilde{G}e^{-i\omega t_L}$, where \tilde{p} is usually decomposed into a direct and a reflected wave, i.e. $\tilde{G} = \tilde{G}_D + \tilde{G}_R$. The direct wave is given by:

$$\tilde{G}_D = -\frac{\gamma^4}{4\pi} \left(ik + Mx_L \frac{ikd_L - 1}{d_L^2} \right) \frac{e^{ikd_L}}{d_L}, \quad (8)$$

with $d_L = \sqrt{x_L^2 + y_L^2 + (z_L - z_{L,S})^2}$ and $z_{L,S} = \gamma z_S$. The reflected wave is obtained as a two-dimensional inverse Fourier transform:

$$\tilde{G}_R = \frac{1}{4\pi^2} \iint_{-\infty}^{+\infty} F(k_x, k_y) e^{ik_x x_L + ik_y y_L} dk_x dk_y. \quad (9)$$

The function F is given by:

$$F(k_x, k_y) = \gamma^4 \frac{k + k_x M}{2\alpha} R(k_x, k_y) e^{i\alpha h_L},$$

with $h_L = z_L + z_{L,S}$ and where R is a reflection coefficient:

$$R(k_x, k_y) = \frac{\alpha Z_S [(\omega + k_x cM)\gamma^2] - (k + k_x M)\gamma}{\alpha Z_S [(\omega + k_x cM)\gamma^2] + (k + k_x M)\gamma}$$

and where $\alpha = \sqrt{k^2 - k_x^2 - k_y^2}$ corresponds to the vertical wavenumber component. Note that the surface impedance Z_S in the reflection coefficient is not a constant and is a function of the wavenumber k_x .

The evaluation of \tilde{G}_R is not straightforward because of the oscillatory nature of the integrand. More specifically, the integrand is oscillatory inside the circle $k_x^2 + k_y^2 \leq k^2$ as α is real. Outside the circle, α is purely imaginary and the integrand is exponentially decaying as k_x or k_y increases. The computation of the integral is performed in two steps. The integral over k_x is first evaluated and then the integration over k_y is performed. As for $|k_y| > k$, α is purely imaginary regardless of k_x , the integration over k_y is computed only for $|k_y| \leq k$. To improve the accuracy and to reduce the CPU time, a Clenshaw Curtis quadrature method [14] is employed. Concerning the integral over k_x , as for $-\sqrt{k^2 - k_y^2} \leq k_x \leq \sqrt{k^2 - k_y^2}$, the integrand is oscillatory, a Clenshaw Curtis quadrature method is again employed. For $|k_x| \geq \sqrt{k^2 - k_y^2}$, the integrand is exponentially decaying and a trapezoidal rule is used.

The time-frequency decomposition obtained from the analytical solution using Eq. (2), (8) and (9) is represented in Fig. 5. A good concordance is observed with the PSD obtained from the numerical solution displayed in Fig. 4. In particular, the amplitude of the PSD is retrieved. In addition, the small destructive interference pattern around $t = 0$ can also be seen on the PSD obtained from the numerical solution.

5. CONCLUSIONS

The radiation of a source moving at a constant height and at a constant speed about an impedance plane was investigated. For that, a time-domain numerical solver of the linearized Euler equations was employed. Two types of ground surfaces were investigated, one being a perfectly reflecting surface and the other one

an absorbing surface. For each case, the numerical solution was compared successfully to an analytical solution. In addition, an analytical solution for a point-source moving at a constant speed and at a constant speed above a finite-impedance surface, based on previous developments, was proposed. As the evaluation of the integral of the reflected wave of the analytical solution requires a large CPU time, future work will focus on its asymptotic evaluation in order to have an accurate evaluation at long range and a fast computation. In addition, the effects of meteorological conditions on the acoustic field due to moving sources will be studied.

Acknowledgement

This work was conducted in the framework of the LabEx CeLyA ("Centre Lyonnais d'Acoustique", ANR-10-LABX-60). It was granted access to the HPC resources of IDRIS under the allocations 2013-022203 and 2014-022203 made by Grand Equipement National de Calcul Intensif (GENCI).

References

- [1] D. Heimann: Wide-area assessment of topographical and meteorological effects on sound propagation by time-domain modeling. *J. Acoust. Soc. Am.*, Vol., Vol. 133, No. 5, 2013, EL 419–425.
- [2] T. Oshima, T. Ishizuka, T. Kamijo: Three-dimensional urban acoustic simulations and scale-model measurements over real-life topography. *J. Acoust. Soc. Am.*, Vol., Vol. 135, No. 6, 2014, EL 324–330.
- [3] R. Mehra, N. Raghuvanshi, A. Chandak, D. G. Albert, D. K. Wilson, D. Manocha: Acoustic pulse propagation in an urban environment using a three-dimensional numerical simulation. *J. Acoust. Soc. Am.*, Vol., Vol. 135, No. 6, 2014, 3231–3242.
- [4] D. Dragna, P. Blanc-Benon, F. Poisson: Modeling of broadband moving sources for time-domain simulations of outdoor sound propagation. *AIAA J.*, Vol. 52, No. 9, 2014, 1928–1939.
- [5] D. Dragna, P. Blanc-Benon: Towards realistic simulations of sound radiation by moving sources in outdoor environments. *Int. J. Aeroacous.*, Vol. 13, No. 5-6, 2014, 405–426.
- [6] T. D. Norum, C. H. Liu: Point source moving above a finite impedance reflecting plane - experiment and theory. *J. Acoust. Soc. Am.*, Vol. 63, No. 4, 1978, 1069–1073.
- [7] K. Attenborough, K. M., Li, K. Horoshenkov: *Predicting outdoor sound*. Taylor & Francis, 2007.
- [8] M. Ochmann: Exact solutions for sound radiation from a moving monopole above an impedance plane. *J. Acoust. Soc. Am.*, Vol. 133, No. 4, 2013, 1911–1921.
- [9] D. Dragna, P. Blanc-Benon: Sound radiation by a moving line source above an impedance plane with frequency-dependent properties. under review for *J. Sound and Vib.*.
- [10] J.-P. Béranger: A perfectly matched layer for the absorption of electromagnetic waves. *J. Comp. Phys.*, Vol. 114, No. 2, 1994, 185–200.

- [11] B., Cotté, P., Blanc-Benon, C., Bogey, F. Poisson: Time-domain impedance boundary condition for simulations of outdoor sound propagation, *AIAA J.*, Vol. 47, No. 10, 2009, 2391-2403.
- [12] D. Dragna, P. Blanc-Benon, F. Poisson: Time-domain solver in curvilinear coordinates for outdoor sound propagation over complex terrain. *J. Acoust. Soc. Am.*, Vol. 133, No. 6, 2013, 3751-3763.
- [13] Y. Miki: Acoustical properties of porous materials: modification of Delany-Bazley models. *J. Acoust. Soc. Jpn.*, Vol. 11, No. 1, 1990, 19-24.
- [14] L. N. Trefethen: *Spectral methods in MATLAB*. SIAM, 2000.